

## Preliminary investigations on picoplankton-related precipitation of alkaline-earth metal carbonates in meso-oligotrophic lake Geneva (Switzerland)

Jean-Michel JAQUET,<sup>1\*</sup> Pascale NIREL,<sup>2</sup> Agathe MARTIGNIER<sup>1</sup>

<sup>1</sup>Section des Sciences de la Terre et de l'Environnement, Université de Genève, 13 rue des Maraichers, CH-1205 Geneva; <sup>2</sup>Service d'Ecologie de l'Eau, Département de l'Intérieur, Mobilité et Environnement (DIME), 23 rue Ste. Clotilde, CH-1211 Geneva, Switzerland

\*Corresponding author: jean-michel.jaquet@unige.ch

### ABSTRACT

In the course of a routine water-quality survey in meso-oligotrophic lake Geneva (Switzerland), suspended matter was collected by filtration on 0.2 µm membranes in July and August 2012 at the depth of maximal chlorophyll a (Chl a) concentration (2 mg m<sup>-3</sup>). Examination by scanning electron microscopy revealed the presence of numerous dark and gelatinous patches occluding the pores of the membranes, containing high numbers of picoplanktonic cells and, in places, clusters of medium-to-high-reflectance smooth microspheres (0.6 µm in diameter). Their chemical composition, determined by semi-quantitative, energy-dispersive X ray spectrometry (EDS) showed magnesium (Mg), calcium (Ca), strontium (Sr) and barium (Ba) (alkaline earth metals) to be the dominant cations. Among the anions, phosphorus (P) and carbon (C) were present, but only the latter is considered here (as carbonate). The microspheres were subdivided into four types represented in a Ca-Sr-Ba ternary space. All types are confined within a domain bound by Ca > 45, Sr < 10 and Ba < 50 (in mole %). Type I, the most frequent, displays a broad variability in Ba/Ca, even within a given cluster. Types II and III are devoid of Ba, but may incorporate P. Type IV contains only Ca. The Type I composition resembles that of benstonite, a Group IIA carbonate that was recently found as intracellular granules in a cyanobacterium from alkaline lake Alchichica (Mexico). Lake Geneva microspheres are solid, featureless and embedded in a mucilage-looking substance in the vicinity of, but seemingly not inside, picoplanktonic cells morphologically similar to *Chlorella* and *Synechococcus*. In summer 2012, the macroscopic physico-chemical conditions in lake Geneva epilimnion were such as to allow precipitation of Ca but not of Sr and Ba carbonates. Favourable conditions did exist, though, in the micro-environment provided by the combination of active picoplankton and a mucilaginous envelope. Further studies are ongoing to investigate the vertical distribution of the microspheres, their internal structure and their exact mineralogical composition, as well as the taxonomy of the picoplankton and the nature of the mucilage, in order to gain a proper understanding of this intriguing process of alkaline-earth metals sequestration.

Key words: Bio-mediated carbonate precipitation, alkaline-earth metals, freshwater, picoplankton.

Received: March 2013. Accepted: June 2013.

### INTRODUCTION

Calcium carbonate (CaCO<sub>3</sub>) precipitation in lacustrine environment is now a well-documented phenomenon. It occurs in hard- to moderately hard-water lakes such as, for example, Constance (Stabel, 1986), Zurich (Kelts and Hsu, 1978) and Bourget (Groleau *et al.*, 2000). An earlier work on lake Geneva showed calcite to be oversaturated in the epilimnion between April and August (Jaquet *et al.*, 1983).

Autochthonous calcite precipitation is dependent on water temperature and pH, the latter increasing with phytoplanktonic primary production. Particulate matter, whether living (plankton and bacteria) or inert (organic or mineral detritus), plays an important role in heterogeneous calcite nucleation, a process at work in natural waters in which saturation index (SI) is too low to trigger homogeneous nucleation (Stabel, 1986).

Picoplankton, as prokaryotic cyanobacteria (*e.g.* *Synechococcus*), or small eukaryotic phototrophs (*e.g.* *Chlorella*), is now recognised as a significant part of

autotrophic plankton in lakes as diverse as Baikal (Belykh and Sorokovikova, 2003), Huron (Fahnenstiel *et al.*, 1991), Tahoe (Winder, 2009) and Maggiore (Callieri and Piscia, 2002). In this last case, it is said to successfully compete with nanoplankton in periods of phosphorus (P) limitation. Picoplankton can be an important actor in CaCO<sub>3</sub> precipitation process, as confirmed by laboratory experiments and field study in lake Lucerne (Dittrich *et al.*, 2004; Dittrich and Obst, 2004). Various strains of *Synechococcus* have been tested for their potential to sequester atmospheric CO<sub>2</sub> (Lee *et al.*, 2006; Jansson and Northen, 2010). This genus has also been found to be active in calcite ooid formation in western lake Geneva (Plée *et al.*, 2008), closely associated to biofilms.

The presence of extracellular polymeric substances (EPS) in biofilms is a key factor in the model of Dupraz *et al.* (2009), which states that organomineralisation can be divided into two coupled elements: i) an alkalinity engine, driven internally by microbial metabolism or externally by the environment (temperature); and ii) an organic

matrix in which mineralisation will take place. Cyanobacteria (Pereira *et al.*, 2009; Dittrich and Sibling, 2010) and some strains of *Chlorella* (Watanabe *et al.*, 2006) are known to secrete extracellular polysaccharides, which may act as binding sites for  $\text{Ca}^{2+}$  and  $\text{CO}_3^{2-}$ . The importance of biofilms in freshwater carbonate precipitation has been demonstrated by Rogerson *et al.* (2008) in their experiments on tufa systems.

In contrast to  $\text{CaCO}_3$ , data on precipitation of other alkaline-earth metals (AEM) such as strontium (Sr) and barium (Ba) are scarcer. This is understandable, as the concentration of these elements in lake water is much lower (molar ratio Ba:Sr:Mg:Ca is of the order of 1:40:1900:8200 in lake Geneva), with saturation indices for Sr and Ba carbonates well below zero under normal physico-chemical conditions.

In the marine environment, biogenic Ba preferably precipitates as sulfate (barite) within dead phytoplankton aggregates (abiotic precipitation) (Jeandel *et al.*, 2000), or under the direct influence of biological processes (Gonzalez-Muñoz *et al.*, 2012).

In lake Constance, Sr has been found to co-precipitate with calcium (Ca) in calcite, while a Ca-independent Sr uptake by biota is negligible (Stabel *et al.*, 1986; Stabel, 1989). According to Stabel *et al.* (1991), the water of this lake is always undersaturated with respect to  $\text{SrCO}_3$  (strontianite), not to mention  $\text{BaCO}_3$  (witherite).

Barium and Sr sulfates (barite and celestite) are known to be present as biominerals in the terminal vacuoles of freshwater Desmids such as *Closterium* and *Micrasterias* (Brook, 1980; Wilcock *et al.*, 1989; Krejci *et al.*, 2011). Barium carbonate (as witherite) has been reported to be precipitated as fibrous crystals by bacteria (Sanchez-Moral *et al.*, 2004). Another avenue for precipitation of AEM is given by the prostomatid ciliates *Loxodes* and *Remanella*, whose müllerian vesicles contain, respectively, Ba and Sr salts (Finlay *et al.*, 1983; McGrath *et al.*, 1989; Lynn, 2010).

It is only recently that a well-identified amorphous carbonate containing magnesium (Mg), Ca, Sr and Ba (attributed to a benstonite-like phase) was found in highly alkaline lake Alchichica microbialites by Couradeau *et al.* (2012). In this case, the carbonate is precipitated as *intracellular* inclusions in a novel cyanobacterium (candidate *Gloeomargarita lithophora*).

Within the framework of ongoing water-quality surveys undertaken by the *Service de l'écologie de l'eau* (SECOE) in Petit-Lac (the southwestern part of lake Geneva), suspended matter was collected in 2012 by filtration at the depth of maximum chlorophyll *a* (Chl *a*) concentration. Examination by scanning electron microscopy (SEM) coupled to energy-dispersive X-ray spectrometry (EDS) revealed, in July and August samples, the presence of Mg-Ca-Sr-Ba-containing microspheres, seemingly related to mucilage packaging picoplanktonic cells.

We present here preliminary investigations conducted by SEM/EDS on the microsphere samples currently available. This study is part of a series of geomicrobiological analyses conducted in lake Geneva (Jaquet *et al.*, 1982; Plée *et al.*, 2008; Glas-Haller, 2010).

## METHODS

Petit-Lac represents the southwest portion of Léman or lake Geneva. After undergoing eutrophication in the 1980s and 1990s (Anneville and Pelletier, 2000), this hard-water lake is now in the process of re-oligotrophication. Data on physico-chemistry, phytoplankton, zooplankton and fish production is available in the French-Swiss Commission yearly reports (CIPEL, 2011; Lazarotto and Klein, 2012). Recent studies on phytoplankton can be found in Anneville *et al.* (2002) and Gallina *et al.* (2011).

Monthly measurements of physico-chemistry and water samples were taken at GE3 station (6.22°E/46.30°N) at 10 different depths ranging 0 to 70 m with a plastic Niskin® bottle. Also, continuous recording of Chl *a* and turbidity was done by means of a Wet Labs® probe (Wet Labs, Philomath, OR, USA). Phytoplankton was collected by means of an integrating sampler over the top 20 m, and taxa were identified and counted following Utermöhl method. A larger water volume (10–15 L) was sampled at the depth of maximum Chl *a* concentration, followed by gentle vacuum filtration in the lab within a few hours on return from the field. For gravimetry, Whatman® GF/F membranes (Whatman Ltd., Maidstone, UK) were used, and Schleicher & Schuell® nitrocellulose (NC 60; 0.6 µm) (Schleicher & Schuell Bio-Science GmbH, Dassel, Germany) as well as Millipore® polycarbonate (PC GTTP; 0.2 µm) (Millipore, Billerica, MA, USA) for SEM/EDS. Filters were air-dried, and no fixation was applied on this first set of samples. Sub-samples of filters were mounted on aluminum stubs covered with double-sided conductive carbon tape. A coating of gold (*ca* 15 nm) or carbon (*ca* 15 nm) was then deposited on the samples prior to imaging with a Jeol® JSM 7001F SEM (Jeol Ltd., Tokyo, Japan) (Department of Earth Sciences, Section of Earth and Environmental Sciences, University of Geneva, Switzerland) with an acceleration voltage of 15 kV. Semi-quantitative elemental analyses were performed with a JED2300 EDS detector (Jeol Ltd.; working distance: 10 mm).

Carbonate species concentrations and calcite saturation index [ $SI = \log(IAP/K_s)$ ] were calculated using the software Aqion 2.5.1 ([www.aqion.de](http://www.aqion.de)), based on USGS PHREEQC (Parkhurst and Appelo, 1999) and the thermodynamical database *wateq4f* (Ball and Nordstrom, 1991).

This preliminary study concerns two suspended matter samples in which microspheres were present. They were collected in 2012: i) on 10<sup>th</sup> July at 6 m depth [polycarbonate (PC) filter numbers 16 and 17, carbon coated] and ii) on 7<sup>th</sup> August at 6 m depth [(PC filters 20, 21 (carbon coated) and 30 (gold coated)]. Clusters of microspheres

were identified visually on the stubs at a magnification of 1000x and numbered as specimens (*Spx\_y-z*, where  $x=1$  for 10.07.12,  $x=2$  for 07.08.12;  $y$ =cluster number and  $z$ =microsphere number).

In order to verify the analytical results obtained by EDS on the microspheres, the mineral benstonite [ $\text{Mg Ca}_6 (\text{Ba}_x\text{Sr}_y) (\text{CO}_3)_{13}$ ] (with  $x+y=6$ ) was synthesised following a modification of Hood and colleagues' procedure (Hood and Steidl, 1973; Hood *et al.*, 1974). The precipitate was aged for three days prior to SEM/EDS analysis. It consists of spherical aggregates of nanoparticles (Supplementary Fig. 1), similar in shape to  $\text{CaCO}_3$  or  $\text{SrCO}_3$  polymorphs reported by Wu *et al.* (2004), Sun *et al.* (2006) and Sondi and Matijevic (2003). The precipitate attribution to benstonite was confirmed by X-ray diffraction (XRD) (Supplementary Fig. 2) and Raman spectroscopy (Supplementary Fig. 3).

## RESULTS

### Limnological context

The microsphere-containing suspended matter samples were collected both times in fairly similar conditions

(Fig. 1a): at 6 m in the metalimnion, corresponding to the peak concentration of Chl *a* ( $2 \text{ mg m}^{-3}$  on both dates) and with a turbidity around 1 NTU.

The water was saturated, with respect to calcite, down to 7 m in July and 10 m in August (Tab. 1, Fig. 1b). Other interesting features are the molar ratios (in solution) Sr/Ca, around 0.0050, similar to lake Constance values as mentioned by Stabel *et al.* (1986), and Sr/Ba, which is higher in the epilimnion (43-45.5; Fig. 1c), practically mimicking the Chl *a* profile (Fig. 1a). Analytical results (Tab. 1) indicate, at 5 m depth, higher temperature, pH, Sr/Ba and calcite saturation values (0.34 vs 0.13) in August. These Sr/Ba maximums were not observed during our other campaigns in 2012 (data not shown).

Fig. 2 shows the phytoplankton groups found in July and August integrated over the top 20 m of the water column. Because of the integration, this may not represent exactly the taxa living at 6 m depth. Moreover, apart from *Chlorella* sp., it does not include picoplankton, which is omnipresent in the SEM images. In terms of biomass, diatoms (Bacillariophyceae) largely dominate in July, with

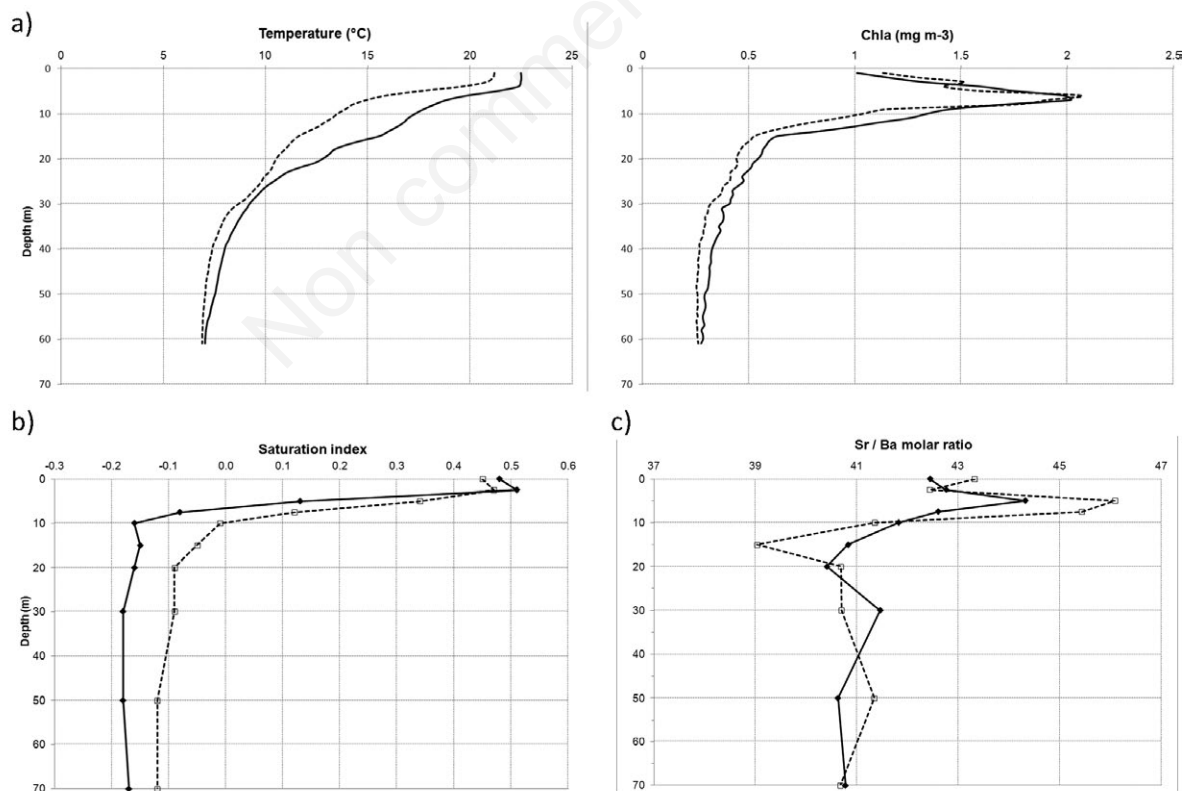


**Fig. 1.** a) Temperature and chlorophyll *a* concentration profiles at GE3 station on 10<sup>th</sup> July (dashed line) and 7<sup>th</sup> August (solid line) 2012; b) corresponding calcite saturation index (samples with saturation index > 0 are saturated with respect to calcite); c) Sr/Ba molar ratio.

lesser amounts of Chlorophyceae, Cryptophyceae and Dinophyceae. In August, the diatoms biomass decreases at the expense of the Chlorophyceae (mostly *Chlorella* sp., with abundance around  $2 \cdot 10^3$  cell mL<sup>-1</sup>). No measurements were carried out for water samples at the Chl *a* maximum. However, for lake Geneva in August (upper 15 m), Personnic *et al.* (2009) report picocyanobacterial abundance values up to  $3 \cdot 10^5$  cell mL<sup>-1</sup>.

### Overall morphology of suspended matter

The general aspect of the suspended matter collected on 10<sup>th</sup> July (concentration: 2.6 mg L<sup>-1</sup>) and 7<sup>th</sup> August (concentration: 1.8 mg L<sup>-1</sup>) is shown in Figs. 3 and 4, respectively. An obvious feature of both samples is the presence of dark patches, very likely of mucilaginous nature, which obliterate the membrane pores.

Low reflectance picoplanktonic cells, either spherical (Fig. 5a, right) or ellipsoidal (Fig. 6a), are densely packed within the mucilage patches. Their dimension is of the order of the  $\mu\text{m}$ . In places, the patches contain clusters of high-reflectance, spherical or subspherical bodies (Fig. 5a), with diameters varying between 0.6 and 3  $\mu\text{m}$ . These

*microspheres* are described in detail below. The mucilage embedding the clusters and picoplanktonic is electronically quasi-transparent, and its limits can be quite sharp and sub-circular (white arrows in Fig. 6a and 6b), suggesting an originally spherical shape prior to the deposition on the filter and subsequent collapse through drying. The presence of this organic matrix is further confirmed by a fortunate feature stemming from electron damage, visible on Fig. 6c: whereas most of the microspheres' contours are blurred by the organic coating (Hernández Maríné *et al.*, 2004), the cracks reveal the presence of underlying, *bare*, sharply delimited microspheres (within white frames in Fig. 6c).

Calcium carbonate is present as isolated crystals (>5  $\mu\text{m}$ ) or aggregates (Fig. 6a), showing signs of corrosion (Fig. 5a). These do not have any visible relationship with mucilage.

In July (Fig. 3), suspended matter contained, in addition to picoplankton, nano- and microplankton (Fig. 2): centric and pennate diatoms and chrysophyte siliceous scales. *Ceratium hirundinella* and diatoms (*Achnanthes* sp.) (Fig. 4) were present in August.

**Tab. 1.** Chemical composition of water at GE3 station (selected elements) and in lake Alchichica aquarium (from Couradeau *et al.*, 2012).

Depth (m)	T (°C)	pH	Alkalinity ( $\mu\text{M L}^{-1}$ )	Mg ( $\mu\text{M L}^{-1}$ )	Ca ( $\mu\text{M L}^{-1}$ )	Sr ( $\mu\text{M L}^{-1}$ )	Ba ( $\mu\text{M L}^{-1}$ )	SI calcite
10.07.2012								
0	20.6	8.52	1570	235	910	5.2	0.12	0.48
2.5	20.0	8.55	1590	235	930	5.2	0.12	0.51
5*	16.0*	8.14*	1730*	235*	1004*	5.3*	0.12*	0.13*
7.5	13.3	7.92	1810	235	1059	5.4	0.13	-0.08
10	12.2	7.86	1820	235	1059	5.3	0.13	-0.16
15	10.6	7.84	1870	240	1094	5.5	0.13	-0.15
20	9.6	7.83	1880	240	1104	5.4	0.13	-0.16
30	7.4	7.84	1880	240	1109	5.5	0.13	-0.18
50	6.4	7.86	1890	240	1104	5.5	0.13	-0.18
70	6.4	7.86	1890	240	1124	5.5	0.14	-0.17
Alchichica aquarium								
	24	8.9	13617	6955	47	0.013	0.001	0.158
05.08.2012								
0	22.4	8.5	1480	232	868	5.0	0.12	0.45
2.5	21.8	8.52	1480	233	882	5.0	0.12	0.47
5*	19.4*	8.38*	1560*	232*	924*	5.0*	0.11*	0.34*
7.5	17.4	8.11	1620	241	994	5.1	0.11	0.12
10	16.4	8	1650	235	986	5.2	0.12	-0.01
15	13.6	7.91	1720	238	1052	5.1	0.13	-0.05
20	11.3	7.89	1790	236	1072	5.2	0.13	-0.09
30	8.2	7.88	1880	249	1145	5.5	0.13	-0.09
50	6.7	7.9	1880	244	1123	5.4	0.13	-0.12
70	6.3	7.9	1880	245	1131	5.5	0.13	-0.12

Mg, magnesium; Ca, calcium; Sr, strontium; Ba, barium; SI, saturation index of calcite (aragonite in Alchichica). \*Approximate depth of occurrence of studied microspheres.

## Alkaline-earth metals precipitates

### Structure

Fifty-five individual microspheres were characterised by SEM and analysed by EDS (Tab. 2). Their morphology can be inferred from SEM photographs in Figs. 5 and 6. They are spherical or sub-spherical and, prior to EDS analysis at least, display a very smooth and featureless surface. Their diameter varies between 0.6 and 3  $\mu\text{m}$ . When struck by the electron beam, a small hole generally appears in the microsphere, which then exhibits damage consisting of cracks and surface alteration (darker punctuations; Figs. 5b and 5c). These features seem to be the expression of bubbles developing inside the microspheres. Notice that adjacent microspheres are also affected, being within the electron beam interaction volume of a few cubic  $\mu\text{m}$  (white circle in Fig. 5b). In some other instances (Fig. 5c), the electron action induces desquamation of the microspheres, which then appear to be composed of several successive layers a few nm thick. In all cases, these bodies seem to consist of a solid, seemingly amorphous substance (at least at the magnification of the SEM, and pending verification by electron diffraction).

### Chemical composition

The microspheres investigated so far have been grouped in five types on the basis of their chemical composition, determined by EDS semi-quantitative analyses

checked by reference to a synthetic benstonite standard. The type numbers and names with averages and minima/maxima are listed in Tab. 2, and the individual microspheres' positions in the Ca-Sr-Ba molar ternary space are shown in Fig. 7. So far, we found 35 microspheres belonging to type I, seven from type II and V, three from type III and only one from type IV. Because of the relatively small sample size (55 clusters), these numbers do not necessarily reflect the true proportion of the various types.

In Tab. 2, the major potential cations are Ca (always present), Ba and Sr, with minor amounts of Mg and potassium (K). Only in type V could P act as a potential anion. However, in this type, there is a severe charge imbalance (Tab. 2, last columns) if P is under the orthophosphate form. This anomaly is hitherto unexplained. In the other groups, we had to postulate the presence of  $\text{CO}_3^{2-}$ , because carbon cannot be validly analysed with the EDS configuration at our disposal. This can be justified by the carbonate hardness of lake Geneva water and by the findings by Couradeau *et al.* (2012), who report the presence of intracellular granules of an unusual benstonite-like phase, a carbonate (Tab. 3, last column) very similar to our microspheres. In the present paper, we shall deal only with types I, II, III and IV (alkaline-earth metal carbonates), setting aside type V to a further study.

Energy-dispersive X-ray spectrometry mapping was carried out to check the distribution of, chiefly, Mg, Ca, Sr and Ba among the various components of suspended matter. An example is given in Fig. 8a (cluster *Sp2\_4*,

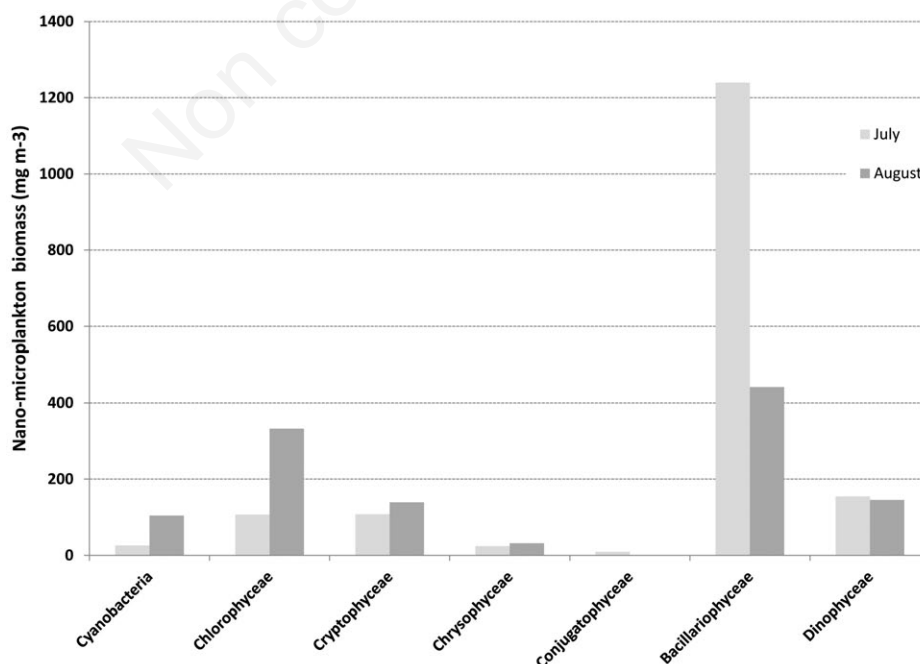


Fig. 2. Biomass of nano-microphytoplankton groups at GE3 station (0-20 m integration) in July and August 2012.

**Tab. 2.** Microspheres average composition (atom %).

Type Name Element	I CaSrBa				II CaSr				III CaPSr				IV Ca		V CaP			
	Mean	N	Min	Max	Mean	N	Min	Max	Mean	N	Min	Max	Mean	N	Mean	N	Min	Max
Mg	0.5	35	0.0	2.2	0.4	7	0.3	0.8	1.2	3	0.8	1.7	1.0	1	3.5	7	1.4	10.6
P	1.2	3	0.0	2.0					5.0	3	3.4				53.5	7	45.0	60.2
S									2.5	1	2.5	2.5			12.4	2	1.3	23.4
K															8.4	2	7.2	9.5
Ca	32.0	35	19.5	64.1	90.1	7	87.0	92.4	82.7	3	76.3	87.5	99.0	1	37.1	7	23.0	43.1
Sr	4.7	35	0.4	10.1	9.5	7	7.3	12.2	10.3	3	6.6	16.0						
Ba	62.8	35	30.7	75.5	0.0	7												
As 100%*																		
Ca	32.2		19.6	64.4	90.5		87.3	92.8	88.9		82.1	94.2	100.0		100.0			
Sr	4.7		0.4	10.1	9.5		7.3	12.3	11.1		7.1	17.2	0.0		0.0			
Ba	63.1		30.9	76.0	0.0				0.0				0.0		0.0			

*N*, number of analyses for a given element; *Min*, minimum; *Max*, maximum; *Mg*, magnesium; *P*, phosphorus; *S*, sulphur; *K*, potassium; *Ca*, calcium; *Sr*, strontium; *Ba*, barium. \*Three last rows: *Ca*, *Sr* and *Ba* normalised to 100%.

**Tab. 3.** Composition (atom %, alkaline-earth elements) of benstonite varieties.

Ratio	(Ba <sub>5.5</sub> Sr <sub>0.5</sub> ) theoretical* 1	(Ba <sub>4.5</sub> Sr <sub>1.5</sub> ) theoretical* 2	(Ba <sub>4.5</sub> Sr <sub>1.5</sub> ) synthetic° EDS	(BaSr) <sub>6</sub> Anthony <i>et al.</i> (2012)	(Ba <sub>2.7</sub> Sr <sub>1.0</sub> Mg <sub>1.4</sub> Ca <sub>0.9</sub> ) Couradeau <i>et al.</i> (2012)
Mg	2.3	2.4	1.3	2.3	18.0
Ca	22.6	23.7	20.8	22.9	53.2
Sr	4.1	13.0	11.2	4.1	8.1
Ba	71.0	60.9	66.7	70.7	20.7

*EDS*, energy dispersive X-ray spectrometry; *Mg*, magnesium; *Ca*, calcium; *Sr*, strontium; *Ba*, barium. \*Computed from formula; °analysed semi-quantitatively by EDS on a polished surface. First row: variable cations, in addition to fixed *Mg*, *Ca*<sub>6</sub>; last column: recomputed from Table S2 in Couradeau *et al.* (2012).

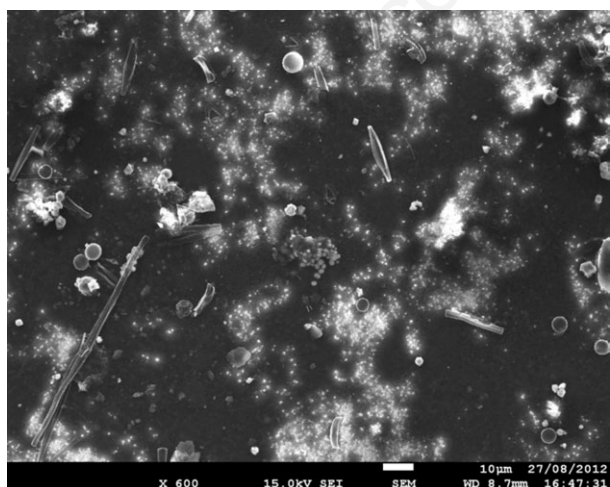


**Fig. 3.** General view of suspended matter from 10<sup>th</sup> July 2012 (6 m depth), deposited on 0.2 µm polycarbonate membrane, carbon coated. Scale bar: 10 µm. Centric and pennate diatoms, CaCO<sub>3</sub> as white aggregates. Darker parts are interpreted as mucilage packaging picoplanktonic cells (see Figs. 5-7 for further details). *Sp1\_1* cluster of microspheres is visible at the centre of the figure.

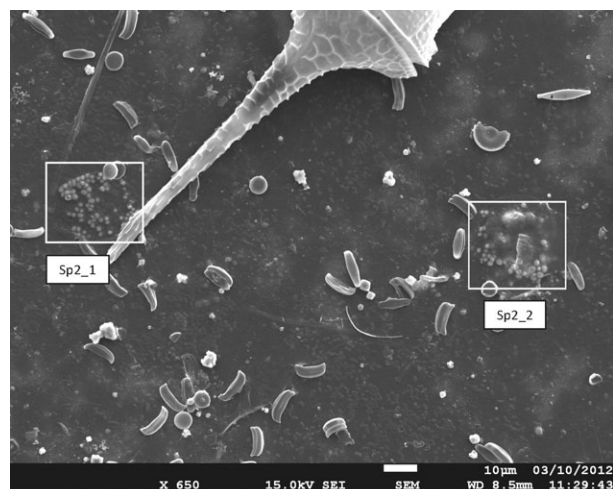


**Fig. 4.** General view of suspended matter from 7<sup>th</sup> August 2012 (6 m depth), deposited on 0.2 µm polycarbonate membrane, gold coated. Scale bar: 10 µm. Apical horn of *Ceratium hirundinella*. Numerous *Achnanthes* sp. diatoms, CaCO<sub>3</sub> are also visible. Darker parts are believed to be mucilage packaging picoplanktonic cells (see Fig. 6a and 6b for further details). Two clusters of microspheres are labelled *Sp2\_1* and *Sp2\_2* (in white frames).

07.08.2012). In this specimen, Ca and Ba are exclusively concentrated in the microspheres, some of which may be rather small. The Sr and silicon (Si) maps are similar due to peak overlaps (Fig. 8b).

## DISCUSSION

### Chemical composition in terms of dissolved alkaline-earth metals

The concentrations of Ca, Sr, Ba and their seasonal variations are quite similar in lake Geneva and lake Constance (Stabel *et al.*, 1991), where these elements are depleted in epilimnion during summer. In lake Geneva, the ratios  $[Me]_{5m}/[Me]_{70m}$  computed from Tab. 1 were, in August 2012, Mg: 0.95, Ca: 0.82, Sr: 0.90 and Ba: 0.85. Hence, it seems that Ca and Ba are slightly more depleted

than Mg and Sr, as an echo to the composition of the microspheres, Ca and Ba representing more than 90% of the cations (Tab. 2) in type I microspheres. In lake Constance, Sr and Ba are said to co-precipitate with calcite at an almost constant stoichiometry in particulate material (molar Sr/Ca=0.0084; atom Sr/Ca=0.018). This could also be the case in lake Geneva, with additional scavenging by the biologically mediated precipitation of specific amorphous AEM carbonates. In contrast, there is no sign of a decrease in Ba concentration towards the bottom (Tab. 1), as in lake Biwa, through adsorption on hydrous manganese oxides (Sugiyama *et al.*, 1992).

### Physico-chemical framework for microspheres precipitation

It is not known whether amorphous AEM carbonate

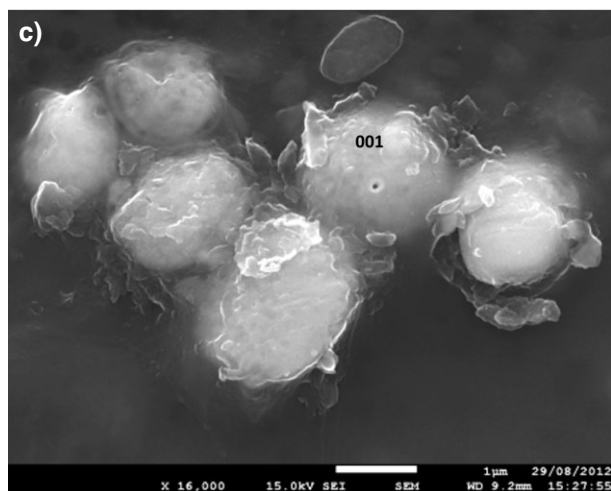
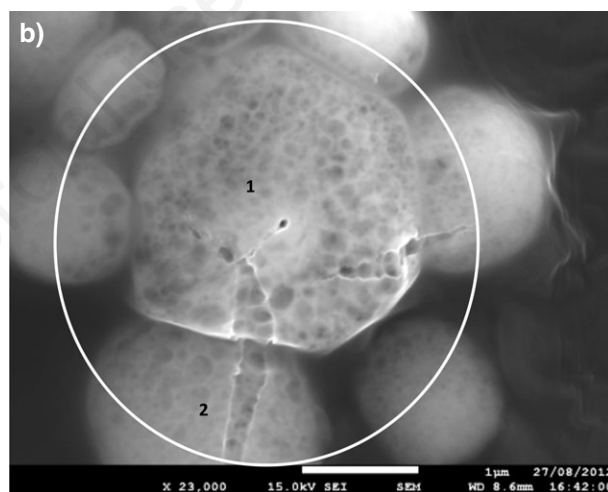
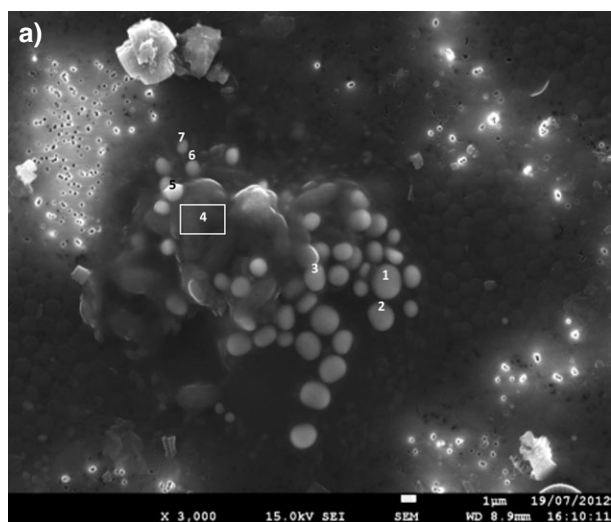


**Fig. 5.** a) Close-up view of microsphere cluster *Sp1\_1* (10.07.2012; from centre of Fig. 3). Scale bar=1  $\mu$ m, carbon coated. Parts of membrane uncovered by extracellular polymeric substances are lighter, with 0.2  $\mu$ m pores well visible. Extracellular polymeric substances-covered parts are darker, and show densely-packed, spherical cells 1  $\mu$ m or less in diameter, with associated microspheres. Numbers refer to individual microspheres that have been analysed by energy-dispersive X-ray spectrometry (EDS) (as points or rectangle). A large  $\text{CaCO}_3$  grain is visible on top. Scanning electron microscopy photograph taken prior to EDS analysis of microspheres (compare with Fig. 5b); b) close-up view of microspheres 1 and 2 in cluster *Sp1\_1* (10.07.2012). Scale bar: 1  $\mu$ m. Scanning electron microscopy photograph taken after EDS analysis. Notice bubbly structure and cracks due to electron ray action within the volume of primary excitation of energy-dispersive X ray spectrometry (EDS) analysis (white circle); c) close-up view of microspheres in cluster *Sp1\_2* (10.07.2012). Scale bar: 1  $\mu$ m. Microspheres seem to consist of several successive pellicles. Notice the hole due to EDS point analysis in *Sp1\_2-001*. Image taken after EDS analysis.

(AAEMC) microspheres existed at other depths and dates than those found by chance in summer 2012. We only know they occurred in the thermocline, near the Chl *a* concentration or biomass maximum, in waters saturated with respect to calcite and at a depth where the dissolved Sr/Ba molar ratio was maximal (Fig. 1). It is, therefore, not unreasonable to postulate that there is a link between microsphere precipitation and phytoplanktonic primary production (PP) (primary production and phytoplankton biomass maxima generally coincide in lake Geneva) (Tadonleke, 2012). This is substantiated by the close spatial association of microspheres and picoplankton visible in SEM images (Figs. 5a and 6a).

If the macroscopic physico-chemical conditions (saturation index > 0; Tab. 1) enable the precipitation of calcite crystals, the situation is different for the AAEMC. Al-

though we were not able to find a value for the solubility constant  $K_s$  of crystalline benstonite (let alone for its amorphous, various species), we can approach the question by considering Stabel *et al.*'s (1991) data: these authors have computed, for lake Constance in summer, the  $[\text{Sr}^{2+}] = 3.16 \cdot 10^{-5} \text{ M L}^{-1}$  and  $[\text{Ba}^{2+}] = 7.08 \cdot 10^{-5} \text{ M L}^{-1}$  concentrations necessary to allow precipitation of strontianite ( $\text{SrCO}_3$ ;  $K_s = 10^{-9.03}$ ) and witherite ( $\text{BaCO}_3$ ;  $K_s = 10^{-8.3}$ ). Extending these figures to our case, it is obvious that Sr and Ba concentrations given in our Tab. 1 are much lower, meaning that these AEM carbonates cannot precipitate under the *macroscopic* pH and temperature conditions in lake Geneva. This is likely to apply also to benstonite-like minerals, the precipitation of which will necessitate micro-environments with extreme conditions (elevated pH, increased ionic concentration and alkalinity).

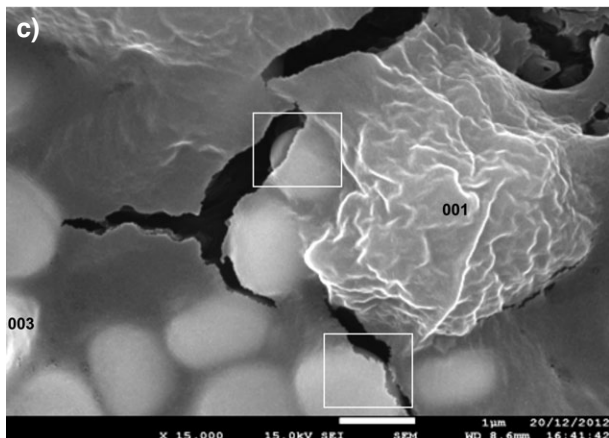
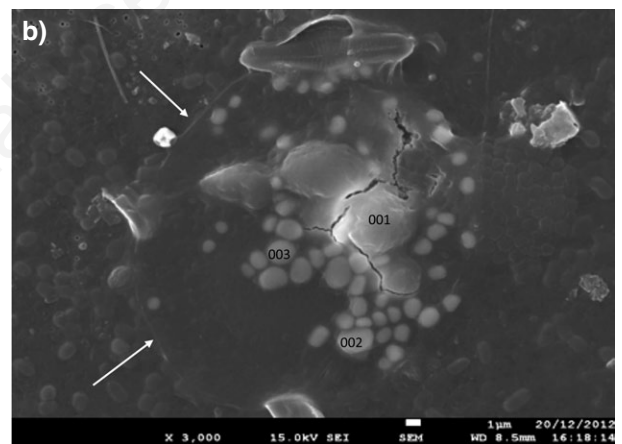
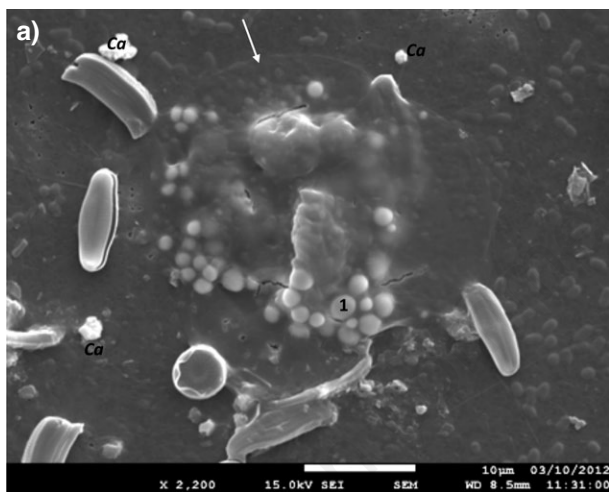


**Fig. 6.** a) View of microsphere cluster *Sp2\_2* (07.08.2012; from right part of Figure 4). Scale bar=10  $\mu\text{m}$ . Most parts of membrane are covered by mucilage (0.2  $\mu\text{m}$  pores not visible), with a well-defined circular mass at centre (upper limit: white arrow). Numerous picoplankton spherical and subspherical cells 1  $\mu\text{m}$  or less in diameter. For analysis of microsphere *Sp2\_2-001* (1 at centre), see Tab. 2. A few  $\text{CaCO}_3$  (*Ca*) grains are visible. Diatoms are *Achnanthes* sp. Photograph taken prior to energy-dispersive X ray spectrometry (EDS) analysis of microspheres; b) view of microsphere cluster *Sp2\_3* (07.08.2012). Scale bar: 1  $\mu\text{m}$ . The microspheres are embedded in a subcircular mucilaginous mass, the left limit of which is quite sharp (arrows). Part 001 is heavily coated with mucilage, whereas 002 and 003 are much less so. Numerous picoplankton spherical and subspherical cells 1  $\mu\text{m}$  or less in diameter. Image taken prior to EDS analysis; c) close-up view of microspheres in cluster *Sp2\_3* (07.08.2012) after EDS analysis. Scale bar: 1  $\mu\text{m}$ . Mucilaginous part 001 has shrunk (compare with Fig. 6b), and the cracks in mucilaginous matrix have widened. In white frames: bare microspheres partially visible under torn mucilage.

## Micro-environment

This micro-environment is provided by the combination of picoplanktonic cells and a mucilage-like matrix in which microspheres have been observed to be embedded. Mucilage or EPS (exopolymeric substances) excreted by micro-organisms consists mainly of polysaccharides, which may contain functional groups for metal binding (Tien, 2002; Dittrich and Sibling, 2006, 2010). For instance, Alvarado Quiroz *et al.* (2006) have reported the strong binding capacity of *sticky* EPS-derived acid polysaccharide compounds for thorium (IV). Likewise, Acharya *et al.* (2009) showed that the ability of *Synechococcus elongatus* to bind uranium was due to its complexation with ligands within the EPS coating cell surface. Extracellular polymeric substances are known to stabilise microbial cells against high-energy environments and to provide a chemically protective microenvironment. They also serve to bind and concentrate  $\text{Ca}^{2+}$  and  $\text{Mg}^{2+}$  ions and raise the alkalinity of the surrounding water (Decho *et al.*, 2005; Couradeau *et al.*, 2012).

Mucilage has not yet been chemically characterised in the samples under study, but we interpret the low reflectance portions of the polycarbonate membranes (Fig. 3) as extra-cellular mucilage because of the following characteristics: obliteration of the 0.2  $\mu\text{m}$  pores (Figs. 5a and 6a); coating of microspheres and presence of numerous picoplanktonic cells (Fig. 6b) in their midst; patch size reaching several tens of micrometers, thereby ruling out their attribution to flattened cells; and, of course, existence of AAEMC precipitates, which were never found *outside* the dark parts of the membranes.

The taxonomic attribution of the picoplankton associated with the mucilage will be clarified in a follow-up study. At the present stage, the densely packed, coccoid cells visible in July sample (Fig. 5a) could be tentatively attributed to two taxa: a member of i) the Chlorellaceae (*Chlorella*, *Dictyosphaerium*) or ii) the Chroococaceae (*Aphanocapsa*, *Aphanothece*). *Chlorella* has been identified in the integrated phytoplankton counts, and these colonial taxa may have mucilaginous envelopes (Bock *et al.*, 2011; Watanabe *et al.*, 2006). Grouped under a *small eukaryotes* category, they have been found in summer in lakes Annecy, Bourget and Geneva (Personnic *et al.*, 2009). The cyanophyta *Aphanocapsa* and *Aphanothece* have also been counted in the integrated phytoplankton sample. In August, most of the micro-organisms found close to the AAEMC microspheres (Fig. 6a) seem morphologically similar to a species of *Synechococcus* (Callieri and Stockner 2002), a cyanobacterium known for its association with EPS (Alvarado Quiroz *et al.*, 2006). Besides, it is possible that *Synechococcus* and *Chlorella* co-exist in the so-called *association Z* reported by Callieri *et al.* (2006) in lake Maggiore. Epifluorescent microscopy, necessary to discriminate between pro- and eukaryotes (Callieri, 2010), could not be done at the time of sampling

in summer 2012. However, water samples collected at the same GE3 station in June 2013 were examined by a combination of SEM and confocal laser scanning microscopy. Under blue excitation we found coccoid and rod-shaped cells appearing yellow [*PE-cells* of Callieri (2010)], and larger (1–2  $\mu\text{m}$ ) cocci emitting in light red (pico-eukaryotes). This finding somewhat supports the taxonomic attribution presented for the summer samples.

On the basis of only SEM images, we cannot know whether the microspheres have precipitated next to, or at the expense of, picoplanktonic cells. The microspheres' aggregation in clusters and their almost perfectly spherical shape would stand in favour of the former alternative, whereas the presence of a pellicle surrounding an internal part might indicate precipitation at the cell surface, as observed by Schultze-Lam and Beveridge (1994) for a *Synechococcus* strain.

## The mineral phase

Medium-magnification SEM images do not reveal any clear features on the microspheres' surface (Fig. 6c). They seem to be solid and compact inside, and the bubbly texture seen in Fig. 5b is an artifact clearly due to EDS analysis. This points towards an amorphous nature for the microspheres, characterising also the AAEMC intracellular granules of lake Alchichica (Couradeau *et al.*, 2012). Interestingly, Addadi *et al.* (2003) stress the role of amorphous  $\text{CaCO}_3$  (ACC or vaterite) in biomineralisation, as temporary storage deposits in various vesicles and transient precursor of calcite or aragonite (Konhauser and Riding, 2012; Mori *et al.*, 2009; Gower, 2008). Finally, similar spherical shapes have been reported in amorphous barite precursors (Gonzalez-Muñoz *et al.*, 2012).

Strictly speaking, types I to IV microspheres should take place in a tetrahedral space with Mg, Ca, Sr and Ba apices to account for the composition given in Tab. 2. However, we have chosen to reduce this representation to a ternary Ca-Sr-Ba system: never exceeding a few atom percents, the Mg analytical results are somewhat doubtful and thus can be temporarily disregarded. The ternary plot of Fig. 7a shows the microspheres to be confined within the domain  $\text{Ca}>45$ ;  $\text{Sr}<10$ ;  $\text{Ba}<50$  (expressed here as %). The Ba/Ca molar ratio varies between 0 and 1.1, indicating a very broad mixture of these cations compared to a relatively narrow Sr variability. In terms of a possible influence of the sampling date on the composition, the domains of occurrence of July and August microspheres on Fig. 7b being separated in places, while overlapping in others, the question cannot be solved for the moment. The plot of Fig. 7c has been used to establish a provisional typology of the microspheres (Tab. 4). The reality of five *discrete* types will have to be checked through the analysis of further microspheres, with consideration of the limited accuracy of EDS analyses. This will establish whether the chemical compo-

sition forms a continuous series. What is clear from Fig. 7c, though, is the impossibility of subdividing type I, as a great variability in the Ba/Ca ratio exists between microspheres *within* a given cluster (represented in the figure as a line joining the squares). Type III differs from type II by

the presence of P and S (Tab. 2). Type IV is, so far, represented by only one individual.

We have attributed type I microspheres to a benstonite-like amorphous phase. The benstonite mineral species is part of the Nickel-Strunz 05.AB Alkali-earth carbonates

**Tab. 4.** Indices of approximate stoichiometric formulae for microspheres.

Microspheres	Mg	Mg <sub>w</sub> Ca <sub>x</sub> (Sr <sub>y</sub> Ba <sub>z</sub> ) (CO <sub>3</sub> ) <sub>13</sub>	Sr	Ba
Type I: average	0.18	7.57	0.55	4.71
Type I: max Ba	0.09	5.76	0.64	6.51
Type I: max Sr	0.24	6.28	1.27	5.21
Type I: min Ba	0.35	10.83	0.31	1.52
Type II: average	0.09	12.31	0.59	0.00
Lake Alchichica	2.4	6.9	1.0	2.7
Benstonite (from Tab. 3)	1.0	6.0	1.5	4.5

Mg, magnesium; Ca, calcium; Sr, strontium; Ba, barium. Lake Alchichica benstonite-like phase stoichiometry is recomputed from Couradeau et al. (2012).

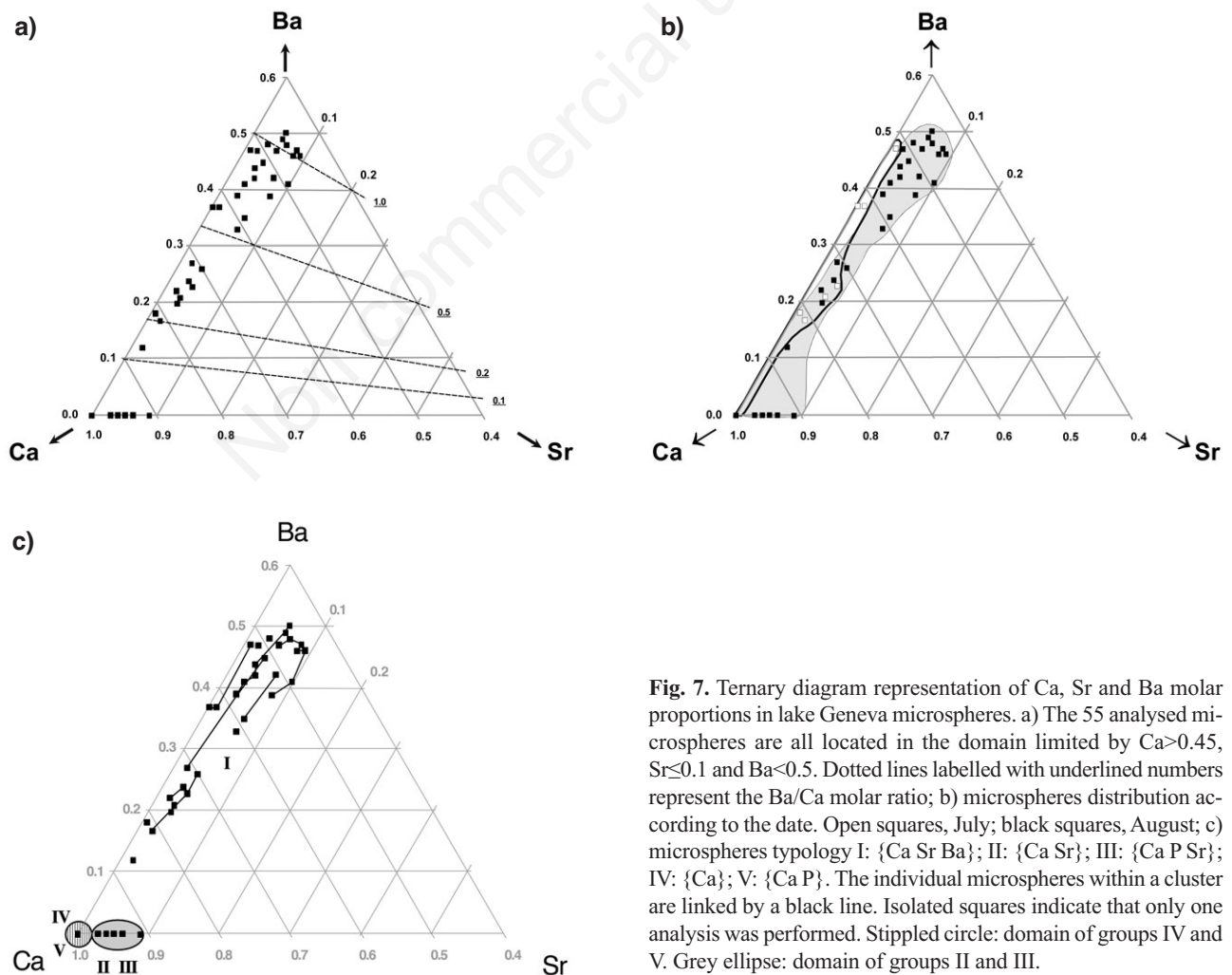


**Fig. 7.** Ternary diagram representation of Ca, Sr and Ba molar proportions in lake Geneva microspheres. a) The 55 analysed microspheres are all located in the domain limited by  $Ca > 0.45$ ,  $Sr \leq 0.1$  and  $Ba < 0.5$ . Dotted lines labelled with underlined numbers represent the Ba/Ca molar ratio; b) microspheres distribution according to the date. Open squares, July; black squares, August; c) microspheres typology I: {Ca Sr Ba}; II: {Ca Sr}; III: {Ca P Sr}; IV: {Ca}; V: {Ca P}. The individual microspheres within a cluster are linked by a black line. Isolated squares indicate that only one analysis was performed. Stippled circle: domain of groups IV and V. Grey ellipse: domain of groups II and III.

category (Barthelemy, 2012; Jolyon, 2012). Its basic formula may be written as  $(\text{Ba},\text{Sr})_6(\text{Ca},\text{Mn})_6\text{Mg}(\text{CO}_3)_{13}$ , with Ba, Sr and manganese (Mn) varying in proportions. In the Magnet-Cove variety (Anthony *et al.*, 2012), the formula is  $(\text{Ba}_{5.27}\text{Sr}_{0.73})\text{Ca}_{6.00}(\text{Mg}_{0.79}\text{Ca}_{0.12}\text{Mn}_{0.09})(\text{CO}_3)_{13}$  or simply  $\text{Ba}_6\text{Ca}_6\text{Mg}(\text{CO}_3)_{13}$ . The variability in composition of different species of benstonite is illustrated in Tab. 3 (from literature) and Tab. 4 (our samples).

In the absence of any significant amount of Mg and Ba, types II, III and IV chemical compositions could be those of an amorphous  $\text{CaCO}_3$  analogous to vaterite with varying amounts of Sr. The molar Sr/Ca ratio in these types of microspheres is around 0.05 (Tab. 5), equal to that found by Lauchnor *et al.* (2013) in microbially induced Ca and Sr co-precipitates. This value lies in the miscibility region of the phase diagram of  $\text{Sr}_x\text{Ca}_{1-x}\text{CO}_3$  solids (Ruiz-Hernandez *et al.*, 2010). As already mentioned, in lake Constance this ratio – computed for well crystallised calcite – is only 0.0084 (Stabel *et al.*, 1991). For ostracod valves in lake Geneva, Sr/Ca never exceeds 0.0025 (Decrouy *et al.*, 2012). These comparisons seem to indicate a higher Sr sequestration potential for the processes producing microspheres.

The EDS analyses being of semi-quantitative nature, caution has to be exercised when comparing our microspheres' composition to that of *mineralogical* or lake Alchichica benstonite-like phase, the latter given as  $(\text{Sr}_{1.0}\text{Ba}_{2.7}\text{Mg}_{1.4}\text{Ca}_{0.9})\text{Ca}_{6.0}\text{Mg}(\text{CO}_3)_{13}$  (Tab. 5, last column). Compared to synthetic benstonite (Tab. 4), lake Geneva microspheres may be higher in Ca (type I, max. Sr and min. Ba), and are always lower in Mg and Sr. All the formulas for *mineralogical* benstonite found in literature have in common an index very close to 6.0 for Ca. This is the case for some lake Geneva type I microspheres, but not for Alchichica granules (6.9). As regard to this and the rather imprecise definition of benstonite, we will consider the attribution of type I microspheres to this mineral phase as tentative only.

Some interesting trends emerge from the element ratios given in Tab. 5. First, the AEM molar ratios are not the same in water and in the microspheres; with respect to Ca, Mg is depressed in the precipitates whereas Sr (average 0.06 in precipitates vs 0.0054 in water) and especially Ba (0.30-0.60 vs 0.00012) are strongly enriched in the microspheres. The dominance of Sr in water (Sr/Ba=44.3) is inverted in type I microspheres (Sr/Ba=0.12). This Ba enrichment is similar to that existing (as barite) in desmids (Wilcock *et al.*, 1989) and marine bacteria (Gonzalez-Muñoz *et al.*, 2012). This could reflect the affinity of Ba for biota (Martin and Knauer, 1973; McGrath *et al.*, 1989).

Some interesting trends emerge from the element ratios given in Tab. 5. First, the AEM molar ratios are not the same in water and in the microspheres; with respect to Ca, Mg is depressed in the precipitates whereas Sr (average 0.06 in precipitates vs 0.0054 in water) and especially Ba (0.30-0.60 vs 0.00012) are strongly enriched in the microspheres. The dominance of Sr in water (Sr/Ba=44.3) is inverted in type I microspheres (Sr/Ba=0.12). This Ba enrichment is similar to that existing (as barite) in desmids (Wilcock *et al.*, 1989) and marine bacteria (Gonzalez-Muñoz *et al.*, 2012). This could reflect the affinity of Ba for biota (Martin and Knauer, 1973; McGrath *et al.*, 1989).

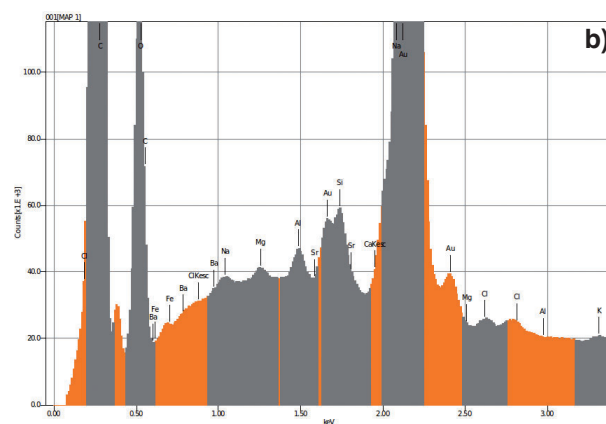
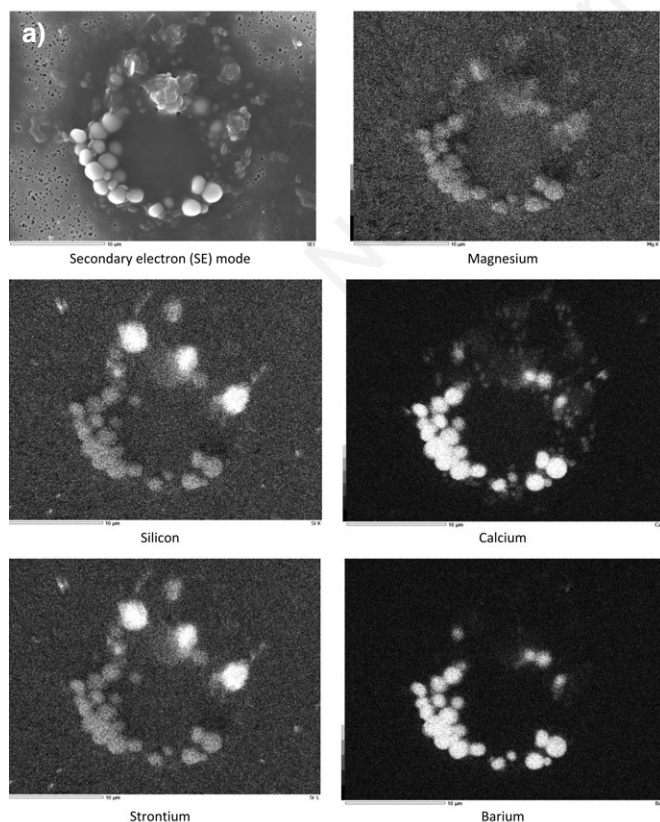


**Fig. 8.** a) Energy-dispersive X ray spectrometry (EDS) mapping of cluster *Sp2\_4* (07.08.2012), embedded in mucilage. Scale bar: 10  $\mu\text{m}$ . Apart from the microspheres, presence of siliceous particles and picoplanktonic cells (1  $\mu\text{m}$  diameter, visible in secondary electron mode). Group IIA metals mineralisation is restricted to bright,  $>2 \mu\text{m}$  microspheres. Strontium map is confounded with silicon (spectral peak overlap). Notice the weaker magnesium signature, matching well the *Sp2\_4 -001* point analysis (not shown); b) Extract of spectrum corresponding to the mapping of cluster *Sp2\_4*. X-axis: energy in keV; Y-axis: counts  $\times 10^3$ . Main peaks are shown in dark grey. Si K (1.73 keV) and Sr L (1.8 keV) peaks are very close.

**Tab. 5.** Selected element atom and molar ratios of water at 5 m depth, in microspheres and various species of benstonite-like phases.

Cation	Water 10.07.2012 5 m	Water 07.08.2012 5 m	Microspheres type I (average)	Microspheres type II (average)	Microspheres type III	(Sr <sub>0.5</sub> Ba <sub>5.5</sub> ) <sup>*</sup> theoretical 1	(Ba <sub>4.5</sub> Sr <sub>1.5</sub> ) <sup>*</sup> synthetic EDS	(Ba <sub>2.7</sub> Sr <sub>1.0</sub> Mg <sub>1.4</sub> Ca <sub>0.9</sub> ) <sup>*</sup> Couradeau <i>et al.</i> (2012)
Mg/Ca <sup>°</sup>	0.14 0.23	0.15 0.25	0.01 0.02	0.01 0.01	0.01 0.02	0.10 0.17	0.06 0.11	0.34 0.56
Sr/Ca	0.012 0.0053	0.012 0.0055	0.15 0.07	0.11 0.05	0.12 0.06	0.55 0.25	0.54 0.24	0.15 0.07
Ba/Ca	0.00041 0.00012	0.00041 0.00012	1.96 0.62	1.01 0.29		2.57 0.75	3.20 0.93	0.39 0.11
Sr/Mg	0.081 0.022	0.078 0.022	9.81 3.10	22.7 6.29	8.56 2.40	5.41 1.50	8.41 2.33	0.45 0.12
Sr/Ba	28.3 44.3	29.4 46.1	0.07 0.12			0.21 0.33	0.17 0.26	0.39 0.61

EDS, energy dispersive X-ray spectrometry; Mg, magnesium; Ca, calcium; Sr, strontium; Ba, barium. <sup>\*</sup>First row: variable cations, in addition to fixed Mg, Ca; <sup>°</sup>top: atom ratio; bottom: molar ratio.

An explanation for the differential enrichment of Sr and Ba in the microspheres could be traced in Rogerson *et al.* (2008), who found that ions other than Ca can be chelated into biofilm EPS, and that this process was highly selective in favour of those ions with small charge density.

Second, with respect to lake Alchichica AAEMC granules, microspheres in lake Geneva are much lower in Mg (Mg/Ca=0.02 vs 0.56) and much higher in Ba (Ba/Ca=0.30-0.60 vs 0.11). This reflects the highly alkaline character of lake Alchichica waters (Tab. 1, bottom row), with high Mg and low Ca, Sr and Ba concentrations.

## CONCLUSIONS

Type I amorphous microspheres (0.6-3 µm diameter) containing Mg, Ca, Sr and Ba found in the epilimnion of lake Geneva in summer 2012 have been tentatively interpreted as a benstonite-like mineral phase. Types II, III and IV, without Ba and with variable Sr, could be ascribed to a vaterite-like phase, a precursor of calcite. All these types are characteristically precipitated within a mucilaginous matrix embedding picoplanktonic cells.

Type I AAEMC microspheres' chemical composition, determined semi-quantitatively by EDS, bears some analogy to that of cyanobacterial intracellular inclusions found in alkaline lake Alchichica (Mexico) microbialites. In lake Geneva, however, the microspheres are pelagic, seemingly extracellular, and contain less Mg but more Ba.

Discovered *a posteriori* in dried suspended matter deposited on filters, these precipitates could be studied only in a preliminary manner. In the context of the little-known Sr and Ba cycles in freshwater, their occurrence raises a series of questions, which will be dealt with in a dedicated study planned for 2013. Is the typology found in 2012 a permanent feature, and how can it be explained? What is

the taxonomic attribution of the picoplanktonic cells spatially associated with microspheres within the mucilage? Precipitating in epilimnion, do the microspheres survive in hypolimnion, and possibly in the sediment? Finally, the internal structure and exact composition of the AAEMC precipitates (as carbonate or phosphate in type V?) and associated mucilage should be investigated with adequate tools in order to gain a proper understanding of this peculiar process of AEM sequestration.

## ACKNOWLEDGMENTS

We are indebted to Sophie Lavigne, who carried out phytoplankton counting and determination. We thank François Gischig, Cédric Schnyder (Muséum d'Histoire Naturelle, Geneva, Switzerland) and Marie-Caroline Pinget (Department of Mineralogy, Université de Genève, Geneva, Switzerland) for preparation, Raman spectroscopy and X-ray diffraction of benstonite samples, respectively. Mathieu Coster was of great help in the synthesis of benstonite. Vincent Ebener and Nathalie Dupont have aptly and faithfully collected samples in the field, and water analyses were carried out by the *Service de l'écologie de l'eau* (SECOE) analytical laboratory. The availability of SEM facilities at the Department of Geology (Université de Genève) is gratefully acknowledged. We are thankful to the reviewers and Journal's editors for their help in improving an earlier version of the manuscript.

## REFERENCES

- Acharya C, Joseph D, Apte SK, 2009. Uranium sequestration by a marine cyanobacterium, *Synechococcus elongatus* strain BDU/75042. *Bioresource Technol.* 100:2176-2181.
- Addadi L, Raz S, Weiner S, 2003. Taking advantage of disorder:

- amorphous calcium carbonate and its role in biomineralization. *Adv. Mater.* 15:959-970.
- Alvarado Quiroz NG, Hung C-C, Santschi P, 2006. Binding of thorium (IV) to carboxylate, phosphate and sulfate functional groups from marine exopolymeric substances (EPS). *Mar. Chem.* 100:337-353.
- Anneville O, Pelletier J-P, 2000. Recovery of Lake Geneva from eutrophication. *Arch. Hydrobiol.* 148:607-624.
- Anneville O, Souissi S, Ibanez F, Ginot V, Druart JC, Angeli N, 2002. Temporal mapping of phytoplankton assemblages in Lake Geneva: annual and interannual changes in their patterns of succession. *Limnol. Oceanogr.* 47:1355-1366.
- Anthony JW, Bideaux RA, Bladh KW, Nichols MC, 2012. Handbook of mineralogy. Mineralogical Society of America ed., Chantilly: 628 pp.
- Ball JW, Nordstrom DK, 1991. User's manual for WATEQ4F, with revised thermodynamic data base and test cases for calculating speciation of major, trace, and redox elements in natural waters. Available from: [http://www.brr.cr.usgs.gov/projects/GWC\\_chemtherm/pubs/wq4fdoc.pdf](http://www.brr.cr.usgs.gov/projects/GWC_chemtherm/pubs/wq4fdoc.pdf)
- Barthelemy D, 2012. Mineralogy database. Available from: <http://webmineral.com/>
- Belykh OI, Sorokovikova EG, 2003. Autotrophic picoplankton in Lake Baikal: Abundance, dynamics, and distribution. *Aquat. Ecosyst. Health* 6:251-261.
- Bock C, Krienitz L, Pröschold T, 2011. Taxonomic reassessment of the genus *Chlorella* (Trebouxiophyceae) using molecular signatures (barcodes), including description of seven new species. *Fottea* 11:293-312.
- Brook AJ, 1980. Barium accumulation by desmids of the genus *Closterium* (Zygnemaphyceae). *Brit. Phycol. J.* 15:261-264.
- Callieri C, 2010. Single cells and microcolonies of freshwater picocyanobacteria: a common ecology. *J. Limnol.* 69:257-277.
- Callieri C, Caravati E, Morabito G, Oggioni A, 2006. The unicellular freshwater cyanobacterium *Synechococcus* and mixotrophic flagellates: evidence for a functional association in an oligotrophic, subalpine lake. *Freshwater Biol.* 51:263-273.
- Callieri C, Piscia R, 2002. Photosynthetic efficiency and seasonality of autotrophic picoplankton in Lago Maggiore after its recovery. *Freshwater Biol.* 47:941-956.
- Callieri C, Stockner JC, 2002. Freshwater autotrophic picoplankton: a review. *J. Limnol.* 61:1-14.
- CIPEL, 2011. General conclusions on the state of Lake Geneva in 2010. Commission Internationale pour la Protection du Léman ed., Nyon.
- Couradeau E, Benzerara K, Gérard E, Moreira D, Bernard S, Brown Jr GE, López-García P, 2012. An early-branching microbialite cyanobacterium forms intracellular carbonates. *Science* 336:459-462
- Decho AW, Visscher PT, Reid RP, 2005. Production and cycling of natural microbial exopolymers (EPS) within a marine stromatolite. *Palaeogeogr. Palaeoclimatol.* 219:71-86.
- Decrouy L, Vennemann TV, Ariztegui D, 2012. Mg/Ca and Sr/Ca of ostracod valves from living species of Lake Geneva. *Chem. Geol.* 314-317:45-56.
- Dittrich M, Kurz P, Wehrli B, 2004. The role of autotrophic picocyanobacteria in calcite precipitation in an oligotrophic lake. *Geomicrobiol. J.* 21:45-53.
- Dittrich M, Obst M, 2004. Are picoplankton responsible for calcite precipitation in lakes? *Ambio* 33:559-564.
- Dittrich M, Sibling S, 2006. Influence of H<sup>+</sup> and calcium ions on surface functional groups of *Synechococcus* PCC 7942 cells. *Langmuir* 22:5435-5442.
- Dittrich M, Sibling S, 2010. Calcium carbonate precipitation by cyanobacterial polysaccharides, p. 51-63. In: H.M. Pedley and M. Rogerson (eds.), Tufas and speleothems: unravelling the microbial and physical controls. Geological Society of London Publ.
- Dupraz C, Reid RP, Braissant O, Decho AW, Norman RS, Visscher PT, 2009. Processes of carbonate precipitation in modern microbial mats. *Earth-Sci. Rev.* 96:141-162.
- Fahnenstiel GL, Carrick HJ, Rogers CE, Sicko-Goad L, 1991. Red fluorescing phototrophic picoplankton in the Laurentian Great Lakes: what are they and what are they doing? *Int. Rev. Hydrobiol.* 76:603-616.
- Finlay BJ, Hetherington NB, Davison W, 1983. Active biological participation in lacustrine barium chemistry. *Geochim. Cosmochim. Ac.* 47:1325-1329.
- Gallina N, Anneville O, Beniston M, 2011. Impacts of extreme air temperatures on cyanobacteria in five deep peri-alpine lakes. *J. Limnol.* 70:186-196.
- Glass-Haller L, 2010. Microbial and geochemical characterization of a contaminated freshwater ecosystem (the case of Vidy Bay, Lake Geneva, Switzerland). University of Geneva ed., Geneva: 186 pp.
- Gonzalez-Muñoz MT, Martinez-Ruiz F, Morcillo F, Martin-Ramos JD, Paytan A, 2012. Precipitation of baryte by marine bacteria: a possible mechanism for marine barite formation. *Geology* 40:675-678.
- Gower L, 2008. Biomimetic model systems for investigating the amorphous precursor pathway and its role in biomineralization. *Chem. Rev.* 108:4551-4627.
- Groleau A, Sarazin G, Vinçon-Leite B, Tassin B, Quiblier-Llobéras C, 2000. Tracing calcite precipitation with specific conductance in a hard water alpine lake (Lake Bourget). *Water Res.* 43:4151-4160.
- Hernández Mariné M, Clavero E, Roldán M, 2004. Microscopy methods applied to research on cyanobacteria. *Limnetica* 23:179-185.
- Hood WC, Steidl PF, 1973. Synthesis of benstonite at room temperature. *Am. Mineral.* 58:341-343.
- Hood WC, Steidl PF, Tschopp DG, 1974. Precipitation of norsethite at room temperature. *Am. Mineral.* 59:471-474.
- Jansson C, Northen T, 2010. Calcifying cyanobacteria. The potential of biomineralization for carbon capture and storage. *Curr. Opin. Biotech.* 21:1-7.
- Jaquet J-M, Favarger P-Y, Peter A, Vernet J-P, 1983. [Premières données sur la matière en suspension dans le Léman]. [Book in French]. Institut Forel, University of Geneva ed., Geneva: 83 pp. Available from: <http://archive-ouverte.unige.ch/vital/access/manager/Repository/unige:27100>
- Jaquet J-M, Nembrini G, Garcia J, Vernet J-P, 1982. The manganese cycle in Lac Léman (Switzerland): the role of *Metallorgenium*. *Hydrobiologia* 91-92:323-340.
- Jeandel C, Tachikawa K, Bory A, Dehairs F, 2000. Biogenic barium in suspended and trapped material as a tracer of export production in the tropical NE Atlantic (EUMELI sites). *Mar. Chem.* 71:125-142.

- Jolyon R, 2012. Mindat.org, the mineral and locality database. Available from: <http://www.mindat.org>
- Kelts K, Hsu KJ, 1978. Freshwater carbonate precipitation, p. 295-323. In A. Lerman (ed.), *Lakes: chemistry, geology, physics*. Springer-Verlag.
- Konhauser K, Riding R, 2012. Bacterial biomineralization, p. 105-130. In: A.H. Knoll, D.E. Canfield and K.O. Konhauser (eds.), *Fundamentals of geobiology*. Blackwell Publ.
- Krejci MR, Wassermann B, Finney L, McNulty I, Legnini D, Vogt S, Joester D, 2011. Selectivity of biomineralization of barium and strontium. *J. Struct. Biol.* 176:192-202.
- Lauchnor EG, Schulz LN, Bugni S, Mitchell AC, Cunningham AB, Gerlach R, 2013. Bacterially induced calcium carbonate precipitation and strontium coprecipitation in a porous media flow system. *Environ. Sci. Technol.* 47:1557-1564.
- Lazarotto J, Klein A, 2012. Physical-chemical changes in the waters of Lake Geneva. Available from: <http://www.cipel.org/wp-content/uploads/2012/11/Evolution-physico-chimique.pdf>
- Lee BD, Apel WA, Walton MR, 2006. Calcium carbonate formation by *Synechococcus* sp. strain PCC 8806 and *Synechococcus* sp. strain PCC 8807. *Bioresource Technol.* 97:2427-2434.
- Lynn DH, 2010. *The ciliated protozoa: characterization, classification, and guide to the literature*. Springer, Amsterdam: 605 pp.
- Martin JH, Knauer GA, 1973. The elemental composition of plankton. *Geochim. Cosmochim. Ac.* 37:1639-1653.
- McGrath M, Davison W, Hamilton-Taylor J, 1989. Biogeochemistry of barium and strontium in a softwater lake. *Sci. Total Environ.* 87/88:287-295.
- Mori Y, Enomae T, Isogai A, 2009. Preparation of pure vaterite by simple mechanical mixing of two aqueous salt solutions. *Mater. Sci. Eng. C29*:1409-1414.
- Parkhurst DL, Appelo CAJ, 1999. User's guide to PHREEQC (version 2): a computer program for speciation, batch reaction, one-dimensional transport, and inverse geochemical calculations. US Department of the Interior ed., denver: 309 pp. Available from: <ftp://brrftp.cr.usgs.gov/pub/dlpark/geochem/unix/phreeqc/manual.pdf>
- Pereira S, Zille A, Micheletti E, Moradas-Ferreira P, De Philippis R, Tamagnini P, 2009. Complexity of cyanobacterial exopolysaccharides : composition, structures, inducing factors and putative genes involved in their biosynthesis and assembly. *FEMS Microbiol. Rev.* 33:917-941.
- Personnic S, Domaizon I, Dorrigo U, Berdjeb L, Jacquet S, 2009. Seasonal and spatial variability of virio-, bacterio-, and picoplanktonic abundance in three perialpine lakes. *Hydrobiologia* 627:99-116.
- Plée K, Ariztegui D, Martini R, Davaud E, 2008. Unravelling the microbial role in ooid formation – results of an *in situ* experiment in modern freshwater Lake Geneva in Switzerland. *Geobiology* 6:341-350.
- Rogerson M, Pedley HM, Wadhawan JD, Middleton R, 2008. New insights into biological influence on the geochemistry of freshwater carbonate deposits. *Geochim. Cosmochim. Ac.* 72:4976-4987.
- Ruiz-Hernandez SE, Grau-Crespo R, Ruiz-Salcedor AR, De Leuw NH, 2010. Thermochemistry of strontium incorporation in aragonite from atomistic simulations. *Geochim. Cosmochim. Ac.* 74:1320-1328.
- Sanchez-Moral S, Luque L, Cañaveras JC, Laiz L, Jurado V, Hermosin B, Saiz-Jimenez C, 2004. Bioinduced barium precipitation in St. Callixtus and Domitilla catacombs. *Ann. Microbiol.* 54:1-12.
- Schultze-Lam S, Beveridge TJ, 1994. Nucleation of celestite and strontianite on a cyanobacterial S-Layer. *Appl. Environ. Microb.* 60:447-453.
- Sondi I, Matijevic E, 2003. Homogenous precipitation by enzyme-catalyzed reactions. 2. Strontium and Barium carbonates. *Chem. Mater.* 15:1322-1326.
- Stabel H-H, 1986. Calcite precipitation in Lake Constance. *Limnol. Oceanogr.* 31:1081-1093.
- Stabel H-H, 1989. Coupling of strontium and calcium cycles in Lake Constance. *Hydrobiologia* 176-177:323-329.
- Stabel H-H, Kleiner J, Merkel P, Sinemus HW, 1991. [Stoffkreisläufe ausgewählter Spurenelemente im Bodensee]. [Article in German]. *Vom Wasser* 76:73-91.
- Stabel H-H, Kuchler-Krischun J, Kleiner J, Merkel P, 1986. Removal of strontium by coprecipitation in Lake Constance. *Naturwissenschaften* 73:551-553.
- Sugiayma M, Hori T, Kihara S, Matsui M, 1992. A geochemical study on the specific distribution of barium in Lake Biwa, Japan. *Geochim. Cosmochim. Ac.* 56:597-605.
- Sun D-M, Wu Q-S, Ding Y-P, 2006. A novel method for crystal control: synthesis and design of strontium carbonate with different morphologies by supported liquid membrane. *Sol. St. Phen.* 39:544-549.
- Tadonleke RD, 2012. Primary production and chlorophyll a biomass in Lake Geneva. *Campagne 2011*:78-84.
- Tien C-J, 2002. Biosorption of metal ions by freshwater algae with different surface characteristics. *Process Biochem.* 38:605-613.
- Watanabe K, Imase M, Sasaki K, Ohmura N, Saiki H, Tanaka H, 2006. Composition of the sheath produced by the green alga *Chlorella sorokiniana*. *Lett. Appl. Microbiol.* 42:538-543.
- Wilcock JR, Perry CC, Williams RJP, Brook AJ, 1989. Biological minerals formed from strontium and barium sulphates. II. Crystallography and control of mineral morphology in desmids. *P. Roy. Soc. Lond. B Bio.* 238:203-221.
- Winder M, 2009. Photosynthetic picoplankton dynamics in Lake Tahoe: temporal and spatial niche partitioning among prokaryotic and eukaryotic cells. *J. Plankton Res.* 31:1307-1320.
- Wu Q-S, Sun D-M, Liu H-J, Ding Y-P, 2004. Abnormal polymorph conversion of calcium carbonate and nano-self assembly of vaterite by a supported liquid membrane system. *Cryst. Growth Des.* 4:717-720.